Construction and Building Materials 444 (2024) 137868

Contents lists available at ScienceDirect

Construction and Building Materials

journal homepage: www.elsevier.com/locate/conbuildmat

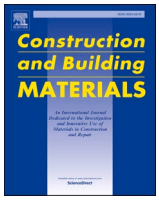

Mechanical strength of rubberized concrete: Effects of rubber particle size, content, and waste fibre reinforcement

Muneeb Qureshi , Jun Li *, Chengqing Wu , Daichao Sheng

School of Engineering and Information Technology, University of Technology Sydney, Sydney, NSW 2007, Australia

ARTICLE INFO

Keywords:
Rubberised concrete
Waste-tyre rubber
Waste-tyre steel-fibres
Mechanical performance

ABSTRACT

Concrete production, ubiquitous in global construction, exerts significant environmental strain, notably through cement manufacturing's carbon footprint and natural sand depletion. As a response, researchers are exploring eco-friendly alternatives, including Waste Tyre Rubber (WTR) aggregates which replace natural sand in concrete. This study investigates the impact of WTR particle sizes (ranging from 0.2 to 4 mm) and volumetric replacements (0–54 %) on Rubberised Concrete Mortar (RuCM) and Rubberised Concrete (RuC) mechanical properties. Additionally, Waste Tyre Steel Fibre (WTSF) reinforcement effects (volume dosage between 0 % and 3 %) are examined and compared with Commercial Steel Fibre (CSF). The study optimizes RuCM and RuC mixes via particle packing theory, incorporating Ground Granulated Blast Furnace Slag (GGBS) and Fly Ash (FA) as cement replacements. Mechanical tests reveal the compressive and flexural strength reduces with an increasing WTR dosage, attributed to the inherent softness of WTR and the weak interfacial bonding between WTR particles and surrounding matrix. Utilizing an optimized RuC mixture with a 10 % WTR replacement yields substantial mechanical improvements, showcasing a remarkable 195 % surge in compressive strength and a noteworthy 61 % elevation in flexural strength over conventional concrete (CC). However, when compared to the control mix devoid of rubber replacement, there is a modest reduction of 16 % in compressive strength and 4 % in flexural strength. Moreover, the incorporation of WTSF reinforcement proves beneficial in mitigating compressive strength losses post rubber particle inclusion and brings about a substantial increase in flexural strength with 3 % volumetric additions. Quantitative analysis reveals the reinforcement effect from WTSF is comparable to the effect of CSF reinforcement. These findings underscore the intricacies and potential opportunities in harnessing WTR and WTSF for the development of resilient and sustainable concrete formulations.

1. Introduction

Concrete, the second most widely utilized material globally, carries a significant environmental impact. The cement manufacturing process alone accounts for approximately 8 % of anthropogenic carbon dioxide emissions and consumes 2–3 % of the world's energy supply, prompting concerns about its ecological footprint. Moreover, the construction sector's substantial demand for natural sand not only strains the environment but also escalates irreparable damage to ecosystems. In response to these challenges, there's a growing impetus among practitioners and researchers in the construction industry to reduce the environmental impact and reliance on natural resources. A key focus has been the development of eco-friendly construction materials by repurposing industrial by-products and waste.

Tyres, recognized as one of the largest landfill waste materials globally, pose significant environmental challenges [1]()(). To counter this, recycling initiatives, particularly within the construction industry, have garnered attention. Notably, rubber particles derived from waste tyres have emerged as a viable replacement for traditional aggregates in concrete mixtures.

Eldin and Senouci [2] pioneered investigations on WTR aggregates in concrete, substituting fine aggregates with WTR sized at 1 mm and coarse aggregates with tire chips ranging between 6 and 38 mm. The results revealed several challenges in rubberised concrete, including low workability, decreased compressive and tensile strengths. These mechanical limitations were attributed to a loss of adherence between the cement matrix and WTR particles, with the size of WTR identified as a primary factor affecting the reduction in material strength. Su et al. (Su et al.) conducted an investigation involving three sets of singly-sized WTR concrete specimens, categorized by WTR particle sizes of 3 mm, 0.5 mm, and 0.3 mm. Their study unveiled that concrete composed of

* Corresponding author.
E-mail address: jun.li-2@uts.edu.au (J. Li).

https://doi.org/10.1016/j.conbuildmat.2024.137868
Received 25 March 2024; Received in revised form 13 July 2024; Accepted 8 August 2024
Available online 9 August 2024

Acronyms

WT	Waste Tyres.
WTR	Waste Tyre Rubber.
WTSF	Copper-coated Waste Tyre Steel Fibre.
CSF	Commercial Steel Fibre.
RuC	Rubberised Concrete.
GGBS	Ground Granulated Blast Furnace Slag.
FA	Fly Ash.
ITZ	Interfacial Transition Zone.
SEM	Scanning Electron Microscopy.
XRD	X-ray diffraction.
SCM	Supplementary Cementitious Materials.
SP	Superplasticizer.
LPDM	Linear Packing Density Model.
SSM	Solid Suspension Model.
CPM	Compressive Packing Model.
PSD	Particle-size Distribution.
CM	Conventional Mortar mix.
GCM	Green Control mix.
RuCM	RuC Mortar mix.
CC	Conventional Concrete.
GCC	Green Control Concrete.
CA	Coarse Aggregates.
HRWR	High-range water reducer.

0.3 mm WTR particles exhibited significantly reduced workability and water permeability due to the larger surface area and higher water absorbability inherent in finer WTR particles. Moreover, as the size of the WTR increased, a reduction in concrete compressive strength was observed. Concrete specimens featuring WTR particle sizes of 3 mm, 0.5 mm, and 0.3 mm demonstrated reductions in compressive strength by 10.6 %, 9.6 %, and 9.5 %, respectively. This decline in strength was linked to the low stiffness and inconsistent surface texture of WTR particles, ultimately weakening the bond between the cement paste and WTR particles. Similarly, Pham et al. [3] prepared RuC with varying WTR sizes of 1–3 mm and 3–5 mm, constituting 15 % volumetric dosage of the mix and revealed RuC incorporating smaller WTR rubber particles exhibited enhanced static compressive strength as compared to those with larger WTR particles. Collectively, these studies underscore the multifaceted challenges and considerations in incorporating WTR aggregates into concrete. The variations in WTR particle sizes, ranging from 0.3 mm to 38 mm bring varying impacts on the workability, water permeability, and compressive strength. While smaller WTR particles demonstrated advantages in compressive strength, challenges such as low stiffness and inconsistent surface texture were identified across different studies. Understanding these intricacies is vital for advancing the development of sustainable RuC formulations in construction practices.

Khaloo et. al. [4] conducted experiments with fine, coarse, and mixed WTR replacement dosages, reaching up to 50 % of the total mineral aggregates' volume in concrete. Their findings revealed that rubberised concrete exhibited lower unit weight and workability in contrast with plain concrete. Higher WTR replacement dosages resulted in a remarkable reduction in concrete's brittle behaviour and an increased toughness index, indicating improved post-failure strength at 25 % WTR replacement dosage. The study also noted that RuC showed a uniform failure state with restricted specimen separation, a reduced crack width and propagation velocity was also noted. The ultimate stress was primarily influenced by the concentration of fine aggregates, while the shape of the stress-strain curve was contingent on the concentration of coarse aggregates. The study suggested that RuC's distinctive behaviour could be further improved by altering the content of fine and coarse aggregates. Ahmad et al. [5] performed an extensive review, encompassing over 100 studies exploring the implications of WTR on the strength, workability, and durability of rubberised concrete. The review underscored the presence of a broad and porous weak Interfacial Transition Zone (ITZ), which negatively impacted the strength of RuC. A notable reduction in strength, ranging approximately from 4 % to 70 %, was observed in concrete featuring rubber content within the range of 5–50 % of natural aggregates. This variation encompasses rubber particles of sizes ranging from 0.075 mm to 6 mm [6] [7]. Thomas and Chandra Gupta [8] through Scanning Electron Microscopy (SEM) testing, confirmed the existence of voids and cracks in the rubber-cement paste interface, highlighting a compromised bonding condition. This weakened bond, coupled with the development of tensile stresses along the surface of rubber particles and the connected cement paste under compressive stress, contributes significantly to the observed strength reduction in RuC, ultimately leading to premature cracking [9].

The weak bonding is attributed to the inherent softness of rubber particles, leading to the initiation of cracks near the junction of rubber and cement paste in concrete. These cracks swiftly propagate, culminating in structural failure. RuC exhibits a conspicuously wide and porous weak ITZ, identified as the concrete mix's weakest section. This is a consequence of the hydrophobic nature of WTR aggregate, which tends to repel cement paste [10]. To address this, potential remedies are developed which include strengthening the bond at the ITZ through practical and cost-effective techniques, incorporating pozzolanic filler additives, and pre-treating WTR particles using methods like NaOH or the silane coating agent process.

Roychand et. al. [11] implemented pre-treatment on WTR particles to enhance cohesion. In the first trial, WTR particle surfaces underwent chemical coating using substances like sodium chloride, sulfuric acid, and potassium permanganate. The second trial involved soaking WTR particles in tap water, while the third trial subjected the particles to heating in an oven before mixing. Post-treated WTR particles were meticulously analysed using x-ray photoelectron spectroscopy to precisely document the chemical composition of WTR surfaces. Scanning electron microscopy further enabled the generation of images of WTR surfaces with atomic-level accuracy. Molecular-scale pre-treatment effects were scrutinized using the afore- mentioned imaging methods, providing researchers with insights into the molecular-scale impacts of each treatment approach on RuC strength and workability. Interestingly, the study observed that water treatment proved more effective than other pre-treatment methodologies, particularly with extended treatment times.

While various rubber pre-treatment methods have shown enhanced bond performance and mechanical properties in RuC, the complex and time-consuming nature of these processes renders them impractical for the concrete industry. Therefore, the quest for an economical and practical method to produce commercially viable WTR is of paramount importance. Water soaking of WTR emerges as a cost-effective approach, devoid of additional chemicals or intricate equipment, providing a streamlined processing method. In a study by Roychand et. al. [11] the effects of soaking WTR in tap water for both short (2 h) and long (24 h) durations were investigated. The study utilized XRD and SEM to analyse compressive strength, bond behaviour, and the rubber/cement ITZ in rubber cement mortar with 20 % sand volume replaced by WTR. The 2-hour soaking duration demonstrated absorbing/adsorbing approximately 80 % of water as compared to the 24 h soaked counterpart. Remarkably, the 2-hour soak not only improved the ITZ between rubber particles and cement paste but also exhibited enhanced 28-day compressive strength in contrast with the 24 h soaked WTR mortar. This reduction in soaking time, coupled with improved strength

properties, holds promise for expediting material handling and construction processes in rubber concrete.

In addition to the rubber pre-treatment, the mineral fillers have been employed to improve the bonding in the ITZ of RuC [8,12]. Turki et al. [13] proposed a solution to elevate the mechanical performance of RuC by introducing mineral fillers like siliceous or limestone alongside rubber. Xie et al. [14] integrated silica fumes with rubber and steel fibres in concrete, achieving commendable strength enhancements, particularly with notable 20 % rubber content. In addition to mineral additives, the pre-treatment of rubber particles using specified solvents or modifiers, such as emulsion or resin, has emerged as a proven methodology, enriching the bonding between rubber and concrete [15]. These artistic interventions contribute to an elevated bond strength within RuC, creating a symphony of robust and reliable mechanical prowess.

Besides the benefits of improving the bonding in RuC, SCMs, such as FA and GGBS also play a pivotal role in concrete mixture. Their contribution extends to filling voids between cement particles, culminating in a reduced water-to-cement ratio at the ITZ, fostering improved coherence with hardened cement paste and elevating packing density [16]. Delving deeper into this realm, Chen et. al. [17] conducted an exploration into enhancing the interfacial behaviour of the rubber-cement matrix within RuC through incorporating SCMs. The findings accentuated that SCMs facilitate a reduction in the W/B ratio of RuC, a strategic move that not only enhances interfacial compactness but also fortifies the bond strength within the rubber-cement matrix interface.

The integration of steel fibre in concrete offers a solution to enhance post-crack ductility and tensile strength, addressing the deficiencies of conventional concrete. Comprising approximately 14–15 % by weight of waste tyres, WTSF has traditionally been utilized as raw material in steel manufacturing and iron feedstock in cement plants. However, recent studies, including those by Bedewi and Nasir [18], showcase the positive impact of WTSF on early-age tensile and flexural strengths in concrete mixtures.

However, Aiello et al. [19] found a slight increase in compressive strength with increasing dosages of WTSF and CSF when the same water quantity was maintained in the concrete mixtures. This finding is supported by Yazici et al. [20] and Atis and Karahan [21], who observed an increase in compressive strength in steel-fibre reinforced concrete (SFRC) with higher steel fibre dosages. This phenomenon can be attributed to the effective contribution of fibre reinforcement confinement, which delays material failure [22]. On the other hand, a reduction in compressive strength can occur due to the physical challenges of achieving a homogeneous distribution of steel fibres within the concrete [23]. Papakonstantinou and Tobolski [24] found that concrete mixtures with steel beads recovered from waste tires were more workable when the fibre content was less than 4 %.

CSF and WTSF are commonly used to enhance various concrete properties, such as impact resistance, toughness ratio [25,26], and ductility [27,28]. Researchers have recently explored the positive synergy between steel fibres and rubberized concrete (RuC). Turatsinze et al. [29] conducted a preliminary investigation to enhance the cracking resistance of concrete, finding that WTR particles, which included steel fibres, improved strain capacity and delayed shrinkage cracks. This combination of steel fibres with WTR shows promise for many concrete engineering applications and could potentially expand the scope of manufacturing such types of concrete in the future [30]. (Ndayambaje) [31] further highlights the optimal performance achieved in RuC with a 12.5 % WTR dosage, coupled with a 1.2 % volumetric fraction of WTSF. The study emphasizes the importance of capping the maximum fibre length at 60 mm to prevent balling effects. In recent investigations, researchers have delved into the potential of utilizing WTSF as a viable alternative to CSF for reinforcing concrete [19,32–34]. The outcomes of these studies suggest that WTSF demonstrate enhanced efficacy in inhibiting the propagation of micro- to meso-cracks, while industrial steel fibres prove more adept at effectively bridging macro-cracks [33,34].

In addition, Pan et. al. [35,36] conducted pioneering research comparing the properties of RuC with Ordinary Portland Cement Concrete (OPC) under static and dynamic conditions. Their findings revealed that RuC with up to 30 % WTR replacement exhibits superior impact resistance under high loading rates. Unlike OPC, which tends to fragment into pieces under impact, RuC remains almost intact, significantly slowing down crack expansion and progressive destruction. In another study by Pham et. al. [37] Geopolymer Rubberized Concrete (GPRuC) was compared to Geopolymer Concrete (GPC). The research showed that the impact resistance of GPC under high loading rates improves with increasing WTR content. At comparable strain rates, GPRuC remained relatively intact, whereas conventional GPC shattered into small fragments. Crack propagation in GPRuC was also significantly slower than in conventional GPC. Pham et. al. [38] also studied Ultra-High-Performance Rubberized Concrete (UHPRuC), substituting silica sand with up to 40 % WTR. This substitution resulted in a reduction in static compressive strength to 67.8 MPa, attributed to the weaker ITZ between WTR and cement and the softer properties of WTR compared to silica sand. However, the compressive strength of UHPRuC was notably higher than that reported in previous research on Normal Strength RuC and High Strength RuC with similar replacement levels. Moreover, the rate of strength reduction in UHPRuC was less pronounced compared to Normal Strength RuC and High Strength RuC at the same rubber content levels.

In conclusion, the exploration of WTR in concrete presents both challenges and opportunities for sustainable construction practices. Various studies have highlighted the varying impact of WTR particle size and content on the workability, water permeability, and compressive strength in RuC. This study employs particle packing theory to optimise RuC mortar and concrete mix designs. The approach involves strategically selecting SCMs like GGBS and FA for cement replacement. The investigation incorporates pre-treatment of WTR, exploring varying particle sizes ranging from 0.2 to 4 mm and different volumetric proportions of WTR (0–54 %), as well as WTSF. These efforts aim to address the weak ITZ and amplify the bond strength within RuC.

2. Experimental programme

This section presents RuC mixture preparation, casting and curing regime and key characteristics.

2.1. Materials

2.1.1. Cement and aggregates

The mixtures utilized general-purpose Portland cement (in accordance with AS 3972), GGBS conforming to AS 3582.2, and FA complying with AS 3582.1. Table 1 provides the physical characteristics of these materials. Local natural aggregates were employed for both fine and coarse aggregates. Fine aggregates consisted of natural dune sand with a particle size of <5 mm and a moisture content of 7.84 %. Coarse aggregates (CA) included single-sized 10 mm and 7 mm CA, with moisture contents of 0.46 % and 0.67 %, respectively. The bulk density of these aggregates typically ranges from 1200 to 1750 kg/m^3, and the fineness modulus (FM) ranges from 6.5 to 8.0. It is noteworthy that both fine and coarse aggregates were produced in accordance with AS 2758.

Table 1
Physical properties and configuration of materials.

Characteristics	Cement	GGBS	FA
Specific Density	3.0–3.2	3.0–3.2	2.35–2.40
Boiling/ Melting Point	>1200 C	>1200 C	>1400 C
pH	>11	>10	

2.1.2. WTR and WTSF

WTR was responsibly sourced from end-of-life automobile and truck tires, acknowledging the variations in physical properties and compositions from different sources. This study specifically utilized WTR particles in the size ranges of 0.2–0.7 mm, 0.2–2 mm, 0.7–2 mm, and 2–4 mm. The particles had a bulk density of 335 kg/m^3, a moisture content of 0.83 %, a specific gravity of 1.15 at 20°C, and a flash point greater than 250°C. These WTR particles were purchased in bulk from a single local supplier in Sydney, Australia, and stored under controlled conditions at the university premises. All preliminary experiments were conducted using material from this source to ensure consistency. The test results reflect the quality of the locally available material, ensuring the study accurately replicates local sourcing conditions.

To enhance the mechanical properties of RuC, WTSF were incorporated. To enhance the mechanical properties of RuC, WTSF were incorporated. These copper-coated fibres, extracted from end-of-life tires, had varying lengths from 25 to 50 mm and thicknesses ranging from 0.15 to 0.40 mm. The tensile strength of these fibres varied from 400 to 1600 MPa. Visual representations of GGBS, FA, WTR, WTSF, and CSF are depicted in Fig. 1.

2.1.3. CSF

In assessing the reinforcement impact on RuC, WTSF was compared with CSF. Two distinct CSFs were included in the tests for comprehensive evaluation. CSF-Medium (CSF-M), was characterized by a length of 35 mm and a diameter of 0.55 mm, an aspect ratio of 65 and a tensile strength of 1345 N/ mm^2. This fibre featured single-hooked both ends bent to enhance bonding. In contrast, CSF-Large (CSF-L) was a hooked-end fibre with a length of 50 mm, a diameter of 1.0 mm, an aspect ratio of 60, and a tensile strength of 1900 N/mm^2. The geometric details of CSFs are visually represented in Fig. 1.

2.1.4. SCMs and superplasticizer (SP)

GGBS and FA were strategically incorporated as partial substitutes for cement in the RuC mixtures. This deliberate inclusion aimed to harness their compound pozzolanic effect, contributing to the overall enhancement of RuC properties [39]. The chemical compositions of these SCMs are comprehensively detailed in Table 2. To achieve the desired workability for various mixtures, a high-range water-reducing admixture was employed.

2.2. RuC mortar and concrete mix design

Various mix design tools are available for designing mortars and concretes, each offering distinct approaches. Notably, the Linear Packing Density Model (LPDM), Solid Suspension Model (SSM), and Compressive Packing Model (CPM) have been postulated based on the properties of multimodal, discretely sized particles [40]. However, these design methods rely on the packing fraction of individual components (such as cement and sand) and their combinations. Incorporating very fine particles into these mix design tools poses challenges, as determining the packing fraction of such fine materials or their combinations is intricate.

An alternative avenue for mix design involves an integral particle size distribution approach for continuously graded mixes. This method offers the advantage of integrating extremely fine particles with relatively less complexity, as elaborated in the subsequent paragraphs.

Establishing a geometrically continuous grading of aggregates in the concrete mixture has been recognized to enhance concrete properties [41]. The work of Fuller & Thompson [42] and Andreasen and Andersen [43] informs that, theoretically, an optimal particle size distribution (PSD) of all the particles in the mix can lead to minimal porosity, as illustrated in Eq. (1).

$$P(D) = \left(\frac{D}{D\max}\right)^q \quad (1)$$

In the equation, $P(D)$ represents the total solids fraction smaller than the size D, where D is the particle size in micrometres (μm), D_{max} is the maximum particle size in micrometres (μm), and q denotes the distribution modulus.

In response to the omission of the minimum particle size in Eq. (1), a modified model has been proposed by Funk and Dinger, expressed as follows: [42]:

$$P(D) = \frac{D^q - D\min^q}{D\max^q - D\min^q} \quad (2)$$

where D_{min} refers as the minimum particle size (μm).

Optimal algorithms derived from the modified Andreasen and Andersen packing model have been successfully applied in designing both normal density and lightweight concretes [44]. Eq. (2) can be employed to design various types of concrete mixtures by adjusting the values of the distribution modulus (q), which quantifies the percentage between fine and coarse particles in the mix. Husken [45] identified the distribution modulus range for optimum packaging between 0 and 0.28. However, according to Brouwers [46], self-compacting concrete (SCC) should be designed with q value ranges between 0.22 and 0.25.

In this study, the optimization of ingredients is facilitated using the modified Andreasen and Andersen model (Eq. (2)). With a fixed q value of 0.23 chosen for mixtures abundant in fine particles, the particle size distribution of selected ingredients is illustrated in Fig. 2. Adjustments to the percentage of each ingredient in the mixture are made until an optimal alignment between the mixture and the targeted curve is achieved, as outlined in Eq. (3). The mixture is deemed optimum when the eccentricity between the targeted curve and the mixture, expressed by the sum of the squares of the residuals (RSS) at distinct particle dimensions, reaches a minimum [47].

$$RSS = \sum_{i=1}^{n} (Pmix(Di^{i+1}) - Ptar(Di^{i+1}))^2 \quad (3)$$

where P_{mix} represents the mixture, and P_{tar} is the aimed grading calculated from Eq. (2).

Steel fibres can disrupt the packing of aggregate particles, significantly increasing the voids between particles, which necessitates more paste to fill these voids and consequently decreases the workability of steel-fibre reinforced concrete (SFRC) [48,49]. To address these issues, the compressible packing model (CPM) proposed by De Larrard [50], which predicts the particle density of multi-particle mixtures under various compaction conditions, was considered by Gong et. al. [51]. They observed two limitations, first, the disturbance effect of steel fibres on aggregate particles cannot be simply evaluated by transforming the fibre into a wall boundary surface, and second, the loosening effect coefficient and wall effect coefficient in conventional CPM are derived by correcting the particle density test data of pure aggregate (without fibre). Additionally, steel fibres not only occupy the volume of the aggregate skeleton and disturb nearby aggregate particles but also negatively affect the interaction between aggregate particles.

Due to the size and shape differences between sand and coarse aggregate, as the volume of fine particles increases, fine sand gradually fills the voids between coarse aggregates until the particle system reaches its densest packing. Beyond this point, with further increases in fine sand, coarse aggregates tend to be suspended in the dominant fine sand, making the wall effect more pronounced and resulting in a decrease in particle density. This observation aligns with the research findings of De Larrard [50] and Bartos et. al. [52].

Regardless of the aggregate combination, the particle density of the pure aggregate mixture is always greater than that of the Fibre-Aggregate mixtures, proving the consistent disturbance and occupation effects of steel fibres on aggregates [53]. According to evaluations of optimal and average particle density, particle densities can be ranked from large to small, showing that steel fibres with larger sizes and higher contents have a smaller effect on the particle density of binary aggregate (BA) mixtures. The size ratio of the binary aggregate and the size

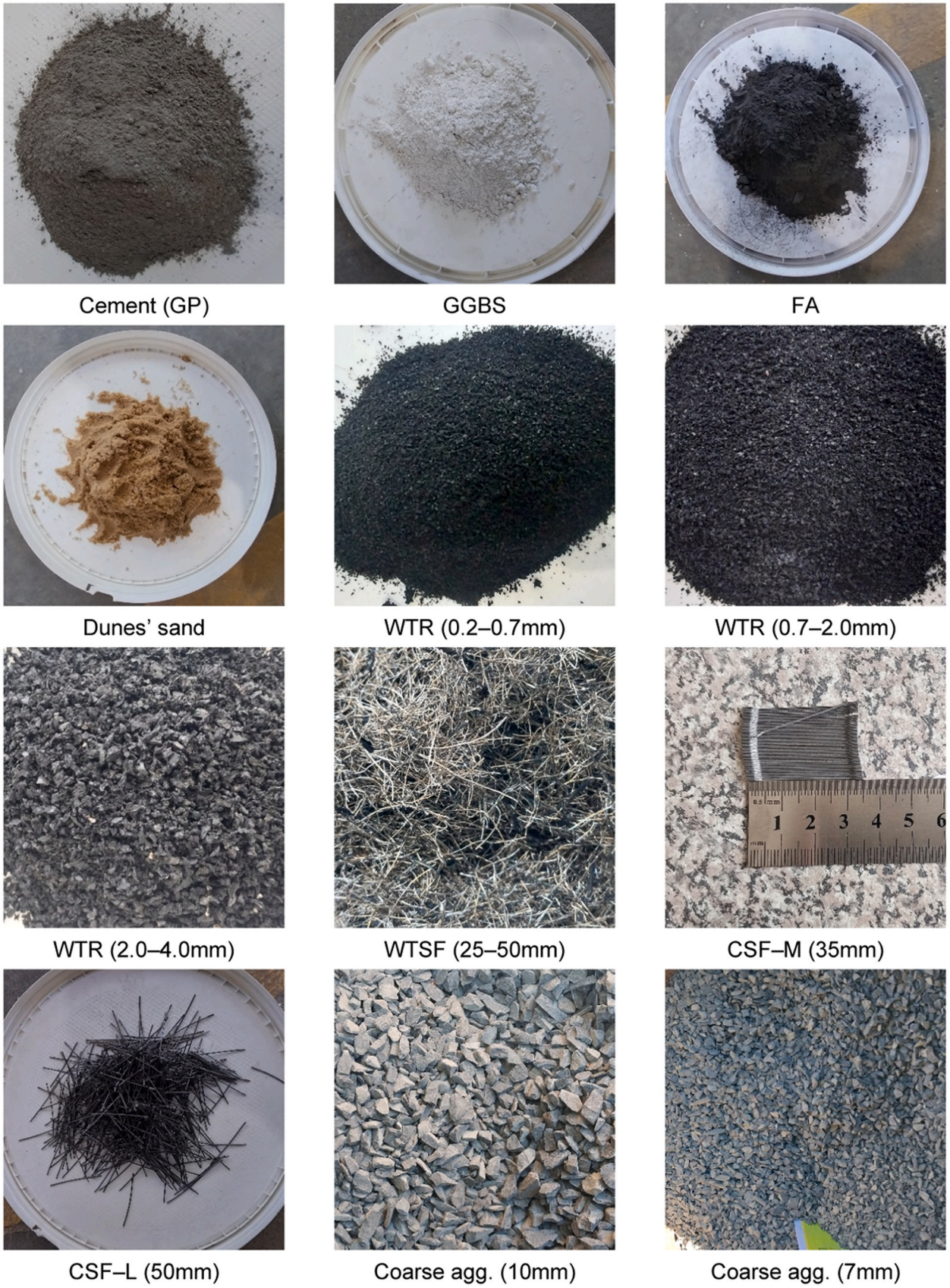

Fig. 1. Raw materials of RuC.

Table 2
The core chemical compositions of SCMs.

Components (wt%)	Cement	GGBS	FA
Portland clinker	>87 %		
Gypsum ($CaSO_4$ 2 H_2O)	2–5 %		
Limestone ($CaCO_3$)	0–7.5 %		
Calcium Oxide	0–1 %		
Hexavalent Chromium Cr (VI)	<10 ppm		≤ 1 ppm
Total respirable silica	Below detection limits		Below reporting limits
Granulated Blast Furnace Slag		>90 %	
Mullite			5–30 %
Crystalline Silica (Quartz)			≤ 5.0 %

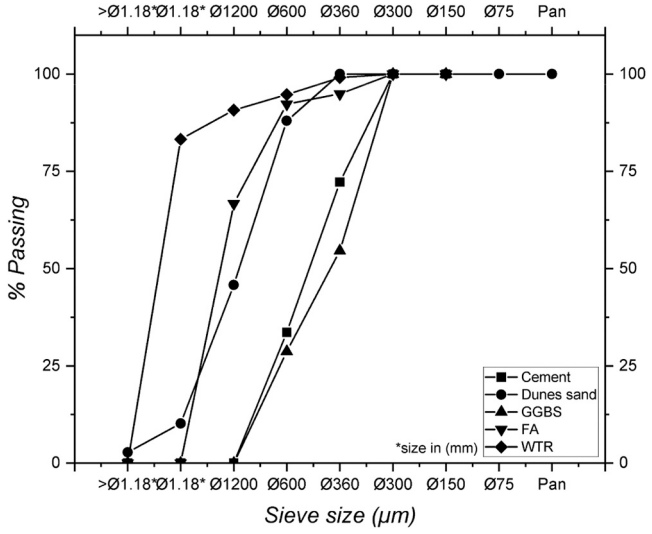

Fig. 2. Particle size distribution of constituents.

features of the steel fibre and binary aggregate are the governing factors.

In this study, the Fibre-BA mixture was determined based on the mixing test results of binary aggregate with a combination of distinct particle classes (10 mm and 7 mm) and steel fibre supplementation up to 3 %. Under a given steel fibre combination, for the two different sizes of coarse aggregates, dune sand combined with WTR, the particle density of the F-BA mixture reached an optimum, and then started decreasing. Within the same binary aggregate mixture (10 mm + 7 mm particles size), the combinations of steel fibres led to noticeable discrepancies in the particle density of each F-BA mixture. This is due to the occupation and perturbation effects of steel fibres on aggregates, as well as the negative effect of steel fibres on the interaction between aggregate particles of different sizes. Finally, combined with the steel fibre, the novel F-BA mixture showed potential for further improvement with higher particle density compared to the conventional mixtures. This research highlights the importance of considering steel fibre size and content, along with the binary aggregate size ratio, in achieving optimal packing density in fibre-reinforced concrete mixtures.

2.2.1. RuC Mortar mix design

The experimental trials initially commenced with weight-based replacements of WTR particles. However, as the investigation progressed the approach was shifted to volumetric replacements instead of weight replacements. This transition aimed to provide a more comprehensive understanding of RuC mixes and was in alignment with most literature studies. To comprehensively investigate the influence of WTR particles as a partial replacement for dune sand in concrete formulations, varying volumes of WTR were precisely incorporated into Rubberised Concrete Mortar (RuCM) mixtures at levels of 9 %, 18 %, 27 %, 36 %, and 54 %. These formulations were designed to offer insights that could assist future research in optimizing RuC mixes. Eshmaiel et al. [54] explored the use of chipped rubber for coarse aggregate replacement and powdered rubber for cement replacement in concrete at 5 %, 7.5 %, and 10 % by weight. Their findings indicated that up to 5 % replacement, the mechanical properties remained similar to the control mix, while significant differences were observed beyond that level. Camille and George [55] studied the use of WTR as fine aggregates in concrete, noting good compressive strength for replacements of less than 25 % WTR, with a substantial drop in strength beyond 25 %. Additionally, Thomas and Gupta [56] investigated the long-term behaviour of RuC and concluded that mixes containing WTR up to 12.5 % exhibited better resistance to water absorption and carbonation. This approach also allowed a comparison against literature study which typically covers a replacement ratio between 10 % and 60 %. Pham et al. [57] experimentally investigated the durability characteristics of RuC with up to 30 % rubber content. They estimated that the service life of 15 % RuC exceeds 50 years, according to fib CEB-FIP and AS 3600 standards. In another investigation, Pham et. al. [58] studied the effects of various pre-treatment methods on WTR and found that WTR-based GPC can serve as a sustainable construction material, offering a path towards cleaner production. It aimed to explore the nuanced effects of WTR dosage considering that strength is more influenced by the total volume of rubber rather than the type of WTR replacement investigated by Raffoul et. al. [12], while seamlessly integrating GGBS and FA as sustainable alternatives to traditional cement. In contrast to conventional mixes (CM), this study introduced the innovative green control mortar mix (GCM). Unlike traditional approaches, GCM replaces 63 % of cement with a strategic blend of 36 % GGBS and 27 % FA. Importantly, this replacement is done without incorporating WTR, thus significantly enhancing the environmental sustainability of the concrete matrix.

The RuCM formulations substituted sand with WTR across a spectrum of replacement levels, ranging from 9 % to 54 %, denoted as RuCM9 to RuCM54, providing a comprehensive overview of the material's performance across varying concentrations. Furthermore, the introduction of WTSF at (78 kg/m^3) 1 % referred as 'WTSF1' and (156 kg/m^3) 2 % referred as 'WTSF2' volume fractions allowed us to explore the synergistic reinforcement effects in RuCM mixtures, with RuCM18-WTSF1 representing an optimized blend with an 18 % WTR replacement reinforced with 1 % WTSF, meticulously detailed in Table 3.

The preparation commenced with dry blending all ingredients, including cementitious materials, for one minute. Pre-treated WTR, soaked in water for 2 hours and dried for 24 hours, was then added and mixed for approximately 3 minutes. Subsequently, 80 % of the water, combined with SP, was introduced, and mixing resumed for 3 minutes until thorough incorporation. The remaining 20 % of water was added and mixing continued for an additional 3 minutes. WTSF was manually dispersed, and wet churning lasted 12–15 minutes until achieving desired consistency, marking the completion of the process.

Post-compaction, the specimens were covered with a thin plastic film for 96 hours to attain initial strength. Subsequently, the specimens were demoulded and cured in an insulated water tank at a temperature of 25°C until mechanical testing. In total 32 mortar mixes and 408 specimens were prepared for assessment of material performance.

Mechanical testing was performed conforming to the Chinese standards GB/T50081–2019 and CECS13–89 at 7 and 28 days of curing. Cubic specimens, measuring (40 × 40 × 40) mm, underwent compression testing utilizing high-precision 500 kN servo hydraulic testing machines. Compression was applied steadily at a rate of 0.7 mm/min until the load fell below 10 % of the peak load, ensuring thorough data collection.

For flexural strength assessment complying with the Chinese standards GB/T50081–2019 and CECS13–89, beam specimens with dimensions of (40 × 40 × 160) mm were subjected to a displacement-

Table 3
Proportions of RuC mortar and concrete mix.

Sample	Cement	GGBS	FA	Sand	Agg. (10 mm)	Agg. (7 mm)	WTR	W/B Ratio	SP	WTSF (Vol. Add.)
RuC Mortar mixes (kg/ m^3)										
CM*	411	–	–	833	–	–	–	0.50	–	–
GCM*	400	400	300	1151	–	–	–	0.30	39	–
RuCM9	400	400	300	1094	–	–	57	0.30	39	–
RuCM18	400	400	300	1046	–	–	105	0.30	39	–
RuCM27	400	400	300	989	–	–	157	0.30	39	–
RuCM36	400	400	300	941	–	–	209	0.30	39	–
RuCM54	400	400	300	836	–	–	314	0.30	39	–
RuCM18-WTSF1/2	400	400	300	1046	–	–	105	0.30	39	78/156
RuCM27-WTSF1/2	400	400	300	989	–	–	157	0.30	39	78/156
RuCM36-WTSF1/2	400	400	300	941	–	–	209	0.30	39	78/156
**Conventional mix (CM) and green control mix (GCM) do not include any WTR replacement.*										
RuC Concrete mixes (kg/ m^3)										
CC0	411	–	–	833	788	523	–	0.50	–	–
GCC0	386	386	289	662	397	265	–	0.24	4.2	–
RuC10	386	386	289	622	397	265	40	0.24	4.2	–
RuC17	386	386	289	596	397	265	66	0.24	4.2	–
RuC10-WTSF1/2/3	386	386	289	622	397	265	40	0.24	4.2	78/156/234
RuC17-WTSF1/2	386	386	289	596	397	265	66	0.24	4.2	78/156

controlled loading protocol at a consistent rate of 0.02 mm/min, maintaining a 100 mm distance between supports. The test proceeded until the load dropped to 10 % of the peak load or the midspan displacement reached 5 mm. These stringent testing procedures ensured reliable and comprehensive characterization of material performance.

2.2.2. RuC concrete mix design

In the current study of RuC concrete, the conventional concrete mix is labelled as (CC), while the green control concrete mix, designated as (GCC), replaces 63 % of cement with GGBS (36 %) and FA (27 %). The rubberised concrete (RuC) mix is essentially a GCC that replaces sand with WTR. A typical specimen label 'RuC10-WTSF1' denotes a 10 % rubber replacement and 1 % fibre reinforcement. Whereas CM and CC0 were designated as conventional C50 mortar and concrete mix samples without incorporating any cementitious materials as cement replacements, WTR as sand replacement, relying solely on the water/binder (w/b) ratio without the addition of superplasticizer (SP) to stabilize the mix. In contrast, all other mortar and concrete samples in this study were specifically fine-tuned and optimized after several trials to balance novel proportions of ground granulated blast-furnace slag (GGBS) and fly ash (FA), which replaced 63 % of the required cement. Additionally, waste tire rubber (WTR) was used in place of dune sand, and the w/b ratio was adjusted and balanced with the introduction of SP. The detailed summary of mixture proportions for the examined RuC concrete compounds is presented in Table 3.

In the preparation of RuC concrete, the procedure commenced with one-minute dry blending of coarse and fine aggregates, followed by the addition of cementitious materials. Subsequently, pre-treated WTR, water soaked and dried, was added to the mix. The mixing process, carefully monitored and controlled, involved staged water additions and manual dispersion of WTSF to guarantee uniform distribution and achieve the desired mix consistency.

After the mixing process, three cylindrical specimens (Φ100 mm×200 mm) and three beam specimens (100 mm×100 mm x 355 mm) were cast. The optimal vibration parameters were determined using the trial-and-error method, considering different percentages of WTR dosages prior to casting the first batch of the mix. Vibration rate and duration were deliberately kept low to avoid any non-uniform dispersion of the matrix aggregate structure.

After compaction, the RuC concrete specimens were cured in the same condition as the mortar specimen. A total of 23 concrete mixes, constituting 276 specimens in total, were prepared to evaluate the mechanical characteristics. The RuC concrete mix with a 10 % volumetric replacement of WTR was identified as the optimal dosage, in contrast to the RuCM mix, where an 18 % volumetric replacement was found to be optimal. In the RuCM mix with a 9 % WTR replacement, the mixer failed to achieve thorough homogeneity, resulting in an 11 % lower compressive strength compared to the optimized RuCM mix with an 18 % WTR replacement. Post-testing examination revealed the presence of smaller lumps of WTR particles, indicating insufficient mixing and mixer limitation due to the quantity of WTR used.

In the RuC mix, the optimal WTR replacement was achieved at 10 % because the presence of coarse aggregates helped break up the smallest lumps of WTR particles, thereby achieving better homogeneity. This level of homogeneity was not fully achievable in the mortar mix. Additionally, a combination of 60 % 10-mm coarse aggregates and 40 % 7-mm coarse aggregates was used instead of the conventional 20-mm coarse aggregate size. This approach considered Johansson's investigation [59], which determined that longer mixing times increased the homogeneity of discharged concrete up to a certain point. The aggregate distribution versus mixing duration curve eventually plateaued, indicating that additional mixing would not enhance the concrete's homogeneity. Johansson's measurements showed that the time to reach this plateau strongly depended on the type of mixer used and was somewhat influenced by the maximum coarse aggregate size. RILEM [60] defines a mixer as efficient when it uniformly distributes all constituents in the container without favouring one over the other. Therefore, evaluating mixer efficiency involves closely monitoring properties such as segregation and aggregate grading throughout the mixture. In addition, Pham et al. [58] identified ultrafine slag (UFS) can effectively compensate for recycled coarse aggregate (RCA) replacing natural coarse aggregate (NCA), enhancing the durability characteristics of GPC. For this study, NCA and RCA of three different nominal sizes (7 mm, 10 mm, and 14 mm) were used. In another study, Pham et al. [61] found that replacing more than 10 % of natural aggregates with rubber aggregates significantly reduces concrete strength. Hence, this combination helped to disperse the lumps more evenly throughout the mix, yielding optimal results for the RuC mix with a 10 % volumetric replacement of WTR.

Mechanical tests, adhering to the guidelines outlined in AS-1012.8.1 (2014), were performed after 7 and 28 days of curing. Cylindrical specimens underwent testing utilizing a 4000 kN servo-hydraulic testing machine. Compression was applied at a consistent rate of 2.62 kN/sec until the load dropped below 10 % of the peak load.

For flexural strength assessment, beam specimens sized at 100 mm×100 mm x 355 mm were subjected to testing in accordance with the specifications outlined in AS-1012.11 (2000), employing a 200 kN universal testing machine. The tests entailed controlled loading at a steady rate of 0.056 kN/sec, while maintaining a clear loading span

of 300 mm, until the load declined to 10 % of the peak load or the midspan displacement reached 5 mm.

3. Results and discussions

3.1. Compressive performance

3.1.1. Mortar

The substitution of fine aggregates with WTR particles of larger size leads to a reduction in mortar strength, as detailed in Table 4. A strength reduction of 68 %, 47 %, and 59 % for RuC mortar with Ø2–4 mm, Ø0.7–2.0 mm, and Ø0.2–2.0 mm particle size was observed when, compared to the same 18 % WTR volume substitution but with rubber sizes between Ø0.2–0.7 mm (RuCM18–Ø0.2–0.7 mm mix). The variation in WTR particle sizes had a notable impact on the outcomes of the RuC mixes. A small variation in WTR particle sizes, ranging from Ø0.2–0.7 mm, yielded significant improvements in performance. However, when the range of WTR particle sizes increased to include both small and medium particle sizes ranging from Ø0.2–2 mm, the outcome diminished considerably by approximately 60 %. Interestingly, when this variation was slightly reduced ranging from Ø0.7–2 mm, the outcome improved, demonstrating a 31 % enhancement with a slight variation of around 0.5 mm in the WTR particle size range.

Conversely, when WTR particle sizes ranged from medium to larger particles, the compressive strength still reduced by 39 %. This reduction, while notable, was 21 % less significant compared to the reduction observed when the particle sizes ranged between small and medium WTR particles. This study highlights the critical importance of controlling WTR particle size variations to optimize the mechanical properties of RuC mixes. The observed strength reduction can be attributed to the lower elastic modulus of WTR in comparison with ordinary fine and coarse aggregates, along with limited bonding between WTR particles and the cement paste [62].

Fig. 3 shows the stress strain curve from specimens with varying WTR particle sizes. Besides evident strength loss, the modulus also exhibits significant reduction. The variation in bonding between different WTR particle sizes and the mixture matrix can induce microfractures, thereby accelerating concrete cracking [54], therefore leading to reduced modulus. Similarly, weak interfacial bonding contributes to the initiation and progression of microcracks around WTR particles. Additionally, Lee [63] noted that the thin layer of air surrounding WTR particles could impede cement hydration, further reducing the strength of concrete. However, the reduction in compressive performance was observed to be less pronounced for finer WTR particles. This can be attributed to the packing effect of finer particles, which reduces the creation of gaps in the paste. Smaller WTR particles exhibited better cohesion with fewer voids than larger particles. The accumulation of WTR particles with sizes between 2.0 and 4.0 mm near the top surface of the casted specimens while settling in the mould is an additional factor contributing to lower strength with coarser particles.

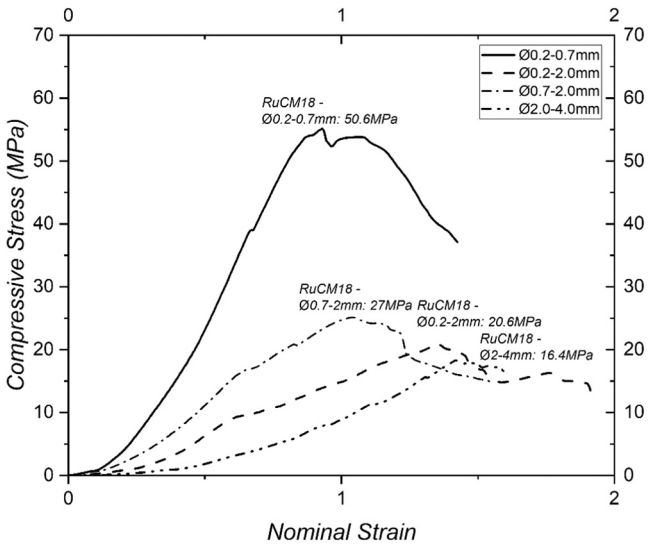

Fig. 3. Comparison of reduction in mortar compressive strengths (at 28-days) with different WTR particle sizes.

The results from the compressive strength tests of RuC mortar specimens with different WTR dosages are presented in Table 5. The columns display the average strength obtained from three specimens of the same mix. It is evident that the compressive performance of RuC mortar mix improved gradually with curing age, but notably decreased with an increase in WTR content. For instance, the 7- and 28-day strengths of specimens with 18 % WTR substitution (RuCM18, the same as the RuCM18-Ø0.2–0.7 mm in Table 4) were 35.6 and 50.6 MPa, respectively. However, the strengths of specimens with 36 % WTR dosage (denoted as 'RuCM36') and 54 % WTR dosage (denoted as 'RuCM54') decreased to 14.3 MPa and 6.7 MPa, respectively, representing reductions of 59.8 % and 81.2 % at 7 days. Similarly, at 28 days, these strengths further decreased to 22.4 MPa and 11.4 MPa, respectively, indicating reductions of 55.7 % and 77.5 %.

The RuC mortar mixture, featuring an 18 % WTR replacement, showcased a reduction of 49.6 % and 23.3 % (50.6 MPa vs. 75.7 MPa and 62.4 MPa) at 28 days in compressive strength as compared to the CM and GCM blends, respectively. As the volumetric replacement of WTR increased to 54 %, there was a substantial decrease in compressive strength, amounting to 39.2 MPa when compared to the optimized RuCM mix. The RuCM mix showed a 52 % reduction in compressive strength as the WTR dosage increased from 0 % to 27 %. This finding aligns with the research by Du, Tianyang et. al. [64], which reported a 40–61 % reduction in compressive strength when WTR content increased from 0 % to 30 %. The hydrophobic properties of rubber result in low interface adhesion between the rubber aggregate and cement

Table 4
Effect of WTR Particles size variations on compressive strength of RuC mortar mix.

Mortar Sample	fc' (MPa)		% Decrease		
			fc'	With reference to RuCM18–Ø0.2–0.7 mm	
	at 7-days	at 28-days	at 28-days	at 7-days	at 28-days
RuCM18-Ø0.2–0.7 mm	35.6	50.6	42 %↑	0 %	0 %
RuCM18-Ø0.2–2 mm	16.7	20.6	24 %↑	−53 %↓	−59 %↓
RuCM18-Ø0.7–2 mm	15.9	27.0	70 %↑	−55 %↓	−47 %↓
RuCM18-Ø2–4 mm	12.0	16.4	37 %↑	−66 %↓	−68 %↓

Table 5
Compressive strengths of RuC mortar mix incorporating varying WTR content.

Mortar Sample	fc' (MPa)		% Increase/ Decrease		
			fc'	With reference to RuCM18	
	at 7-days	at 28-days	at 28-days	at 7-days	at 28-days
CM0	38.2	75.7	98 %↑	7.3 %↑	49.6 %↑
GCM0	42.4	62.4	47 %↑	19.1 %↑	23.3 %↑
RuCM9	24.6	45	83 %↑	−30.9 %↓	−11.1 %↓
RuCM18	35.6	50.6	42 %↑	0.0 %	0.0 %
RuCM27	19.7	30.2	53 %↑	−44.7 %↓	−40.3 %↓
RuCM36	14.3	22.4	57 %↑	−59.8 %↓	−55.7 %↓
RuCM54	6.7	11.4	70 %↑	−81.2 %↓	−77.5 %↓

paste, leading to a reduction in strength. The reduction in compressive strength was more pronounced with larger WTR particles compared to smaller ones. Similar to the influence of WTR particle size, it is significant to note that a higher WTR substitution in the mixture correlates with a decline in compressive performance, encompassing both strength and modulus, as delineated in the stress-strain curve illustrated in Fig. 4. However, concurrently, it enhances the ductility of the specimen, allowing it to bear loads for an extended period.

The WTR dosage has a notable impact on mortar compressive strength, with detrimental effects becoming more pronounced as the dosage of WTR increases. This decrease in compressive strength is associated with three key factors: (a) deformation of WTR particles as compared to the neighbouring cement microstructure, leading to the initiation of cracks correlated with air pockets, (b) weak interfacial connection between WTR particles and the cement matrix, and (c) potential reduction in the density of the mixture matrix based on the size, density, and toughness of WTR particles [12,65,66].

Several iterations were conducted to fine-tune the proportions of cement, SCMs, and fine aggregates for the RuC mortar mixes. Following meticulous experimentation, the RuC mortar mix was optimized at a ratio of 1 part (cement + GGBS + FA) to 1.05 parts fine aggregates. The addition of a SP remarkably bolstered the strength of the RuC mortar mix. Trials were executed to ascertain the optimal dosage of a high-range water reducer (HRWR), culminating in optimization at a dosage of 3.5 % in conjunction with a highly effective water-binder (W/B) ratio of 0.30. This systematic methodology ensured precise adjustments in both SP dosage and W/B ratio, thereby contributing to the formulation of the optimal RuC mortar mix.

3.1.2. Concrete

Following the mortar study, RuC concrete was prepared. The optimization of RuC mix presented several challenges, particularly when incorporating coarse aggregates into the mortar mix during the development of a new RuC mix. The developed RuC mix aligns with the particle packing density theory, maintaining the identical q value of 0.23. A total of eleven (11) trials were conducted, encompassing 23 different concrete mixes and 276 samples, to address these challenges and refine the mix design. Key challenges included:

3.1.2.1. Balancing proportions. The initial RuC mix ratio (1-part cement, GGBS, and FA to 2-part fine aggregates to 4-part coarse aggregates) proved unworkable, as specimens could not be casted with the selected water/binder (w/b) and superplasticizer (SP) proportions, even after 96 hours. This necessitated discarding the materials. Alternative ratios such as 1:1.8:2.7, 1:1.5:3, and 1:2:2.7 were explored. Through iterative adjustments, the optimal mix was identified as 1-part cement, GGBS, and FA to 1-part fine aggregates to 1-part coarse aggregates, which allowed demoulding after 24 hours—a feat not achievable with the earlier trials, even after 96 hours.

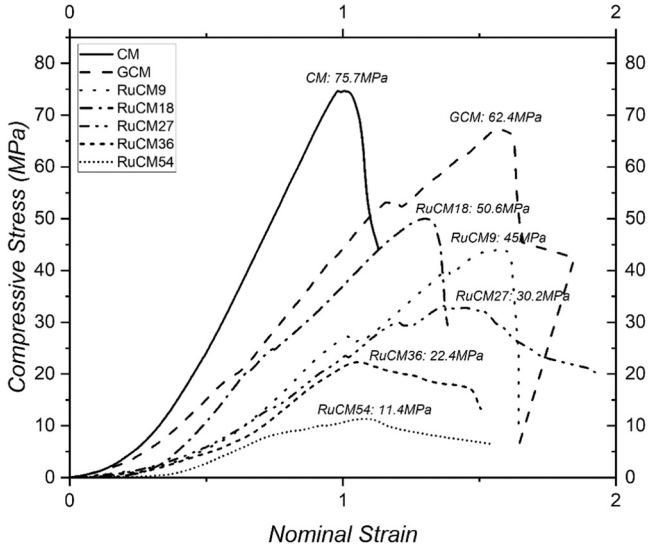

Fig. 4. Variation in mortar compressive strengths (at 28-days) with different WTR particle content (0 %, 9 %, 18 %, 27 %, 36 %, 54 %).

3.1.2.2. Integration and homogeneity. Achieving proper integration of WTR particles and uniform homogeneity posed significant challenges. Initial trials revealed that WTR particles did not mix properly, forming a thin layer of black water on the surface of freshly poured concrete in the moulds. Over time, larger particles accumulated in this layer, creating a thick deposit that had to be manually removed after demolding. Post-demolding analysis showed that the mix matrix stabilized in distinct layers: the finest particles on top, a major portion containing cement, GGBS, and FA particles in the middle, a blend of sand particles below that, and coarse aggregates settled at the bottom. Although subsequent trials improved the mixture, they still resulted in a major portion containing a blend of cement, cementitious materials, and fine aggregates, with some coarse aggregates settling at the bottom. Trial attempts continued until homogeneity was achieved, as post-testing analysis eventually revealed an even dispersion of cement, cementitious materials, fine, and coarse aggregates from top to bottom throughout the casted specimens.

3.1.2.3. Optimizing the quantity of SP and W/B ratio. Multiple trials were conducted to fine-tune the proportions of cement, fine aggregates, and coarse aggregates for RuC mixes, with a particular focus on the role of superplasticizers (SP) in enhancing strength and stabilizing the mix. Initial trials began with a high-range water reducer (HRWR) at 10.5 % and an increased water-to-binder (w/b) ratio. These trials failed, as the material remained unset in the mould for up to 96 hours. Subsequent trials tested HRWR proportions of 5.13 %, 3.75 %, 2.57 %, and 1.25 % with corresponding w/b ratios of 0.33, 0.30, 0.26, and 0.22. Although these mixes allowed for casting, they exhibited issues with WTR particles floating to the surface and coarse aggregates settling at the bottom. These mixes showed inferior compressive and (flexural strengths), with values such as 20.3 MPa (6.3 MPa), 24.1 MPa (5.2 MPa), 29.8 MPa (7.3 MPa), and 78.1 MPa (7.6 MPa). Despite these issues, the matrix formation began to show increased density, partially retaining WTR particles and coarse aggregates.

As the proportions of SP and w/b were adjusted, the floating of WTR particles ceased, but the mix still experienced segregation. Further trials with HRWR proportions of 0.63 %, 0.60 %, 0.50 %, and 0.40 %, and w/b ratios of 0.26, 0.24, 0.23, and 0.22, progressively addressed these segregation issues while influencing the workability of the concrete mix. Optimization was achieved at an SP dosage of 0.4 % with a w/b ratio of 0.24. This systematic approach, involving precise adjustments in both SP dosage and w/b ratio, led to the formulation of the optimal RuC mix.

The RuC concrete mix with a 10 % volumetric replacement of WTR (as opposed to the mortar mix with an 18 % volumetric replacement of WTR) was determined to be the optimum dosage. This choice was based on the understanding that the presence of coarse aggregates assists in breaking up the smallest lumps of WTR particles, a feat that was not fully achievable in the mortar mix. A combination of 60 % with 10-mm coarse aggregates and 40 % with 7-mm coarse aggregates was found to yield optimal results for the RuC mix with a 10 % volumetric replacement of WTR. The decrease in RuC strength due to the inclusion of WTR can be explained by several factors: (a) Modulus of Elasticity (MoE) Disparity: Rubber and concrete have significantly different moduli of elasticity (MoE) [67]. The elastic modulus of concrete is about 5000–24,000 times that of rubber. This disparity makes RuC prone to cracking around the rubber particles during the loading process, thereby accelerating the damage to the concrete, and (b) Aggregate Grading Disruption:

Aggregates play a crucial role in providing structural integrity to concrete, akin to a human skeleton. Proper grading helps the concrete achieve an optimal state. The introduction of rubber disrupts the grading between the sand and aggregate, negatively impacting the structural integrity and strength of the concrete [68].The optimized RuC concrete mix exhibited a substantial 195 % increase in compressive strength when compared against base conventional concrete (CC), and only a marginal 14 % lower strength as compared to the green control concrete (GCC) without any WTR replacement as depicted in Fig. 5.

3.1.3. Mortar incorporating steel fibres

The WTSF derived from discarded car and truck tires exhibited diverse thicknesses and lengths, ranging between 0.15–0.40 mm and 25–50 mm, respectively. Extracted from used tires, these WTSF displayed curvature and bends, with some still partially covered by remnants of waste tire material. Additionally, certain WTSF was found clustered together, requiring separation at the time of incorporation into the mixture. In contrast, CSF maintained consistent thickness and length, featuring bends and flat ends at both sides.

The results presented in Table 6 suggest that incorporating both WTSF and CSF has an adverse effect on the compressive strength of RuC mortar mixes when the rubber particle content is low at 18 %. With the increase in rubber particle content, i.e., the matrix with more inherent defects, the fibre reinforcement provided evident benefit. Zamei [69] reported that incorporating steel fibres in concrete positively impacts compressive and flexural strength. Additionally, three different shapes of CSF (straight, corrugated, and hooked-end) were evaluated, with hooked-end CSFs showing the best performance. Therefore, in this study, hooked-end CSFs were compared with WTSF.

The results indicate that incorporating WTSF has an adverse effect on the compressive strength of the RuCM18 mix. For the compressive strength tests, prism specimens measuring 40 ×40 ×40 mm were casted. During casting, the varied lengths and diameters of the WTSF caused the fibres to disperse in different directions (vertical, diagonal, and horizontal), with some fibres forming lumps due to entanglement during the extraction process, along with remnants of WTR particles. This hindered strong bonding with the cement matrix, creating weak zones, air pockets, and areas where the WTSF was parallel to the applied load during testing. These factors contributed to the earlier failure of the specimens, resulting in inferior compressive strength compared to the same mix without WTSF.

In contrast, the specimens casted for flexural strength tests were beam-shaped, measuring 40 x 40 x 160 mm, and tested under three-point bending. The longer dimensions of the beam allowed more area for the WTSF to settle horizontally, positioning them perpendicularly to the applied load during testing. Compared to the prism samples used for compressive strength tests, the beams' longer dimensions provided a greater area to distribute the applied load across the specimen. This orientation and the increased area for load distribution resulted in higher flexural strength for the mixes with WTSF compared to those without. The WTSF effectively resisted the tensile stresses induced during the bending tests, enhancing the overall flexural performance.It is worth noting that WTSF reinforcement, denoted as WTSF1 (1 % fibre) and WTSF2 (2 % fibre), consistently provided better reinforcement effects as compared to commercial new fibres CSF-M and CSF-L. The numeric digit at the end of WTSF, CSF-M, and CSF-L indicates the fibre percentage, highlighting the varying levels of reinforcement achieved with different fibre compositions. A possible explanation is the WTSF fibres with random length and diameter are capable of inhibiting cracks with wide range of the width, thus effectively retard the formation of macro cracks in the specimen, leading to better load carrying capacity. Further discussion on fibre reinforcement effect is presented later in the flexure behaviour.

Table 6
Compressive strengths of RuC mortar mix reinforced with WTSF and CSF.

Mortar Type	fc' (MPa)		% Increase/ Decrease	
			With reference to RuCM18, RuCM27 and RuCM36, respectively.	
	at 7-days	at 28-days	at 7-days	at 28-days
RuCM18	35.6	50.6	0 %	0 %
RuCM18-WTSF1	18.7	39.3	−47 %↓	−22 %↓
RuCM18-WTSF2	30.3	37.0	−15 %↓	−27 %↓
RuCM18-CSF-M1	27.0	33.6	−24 %↓	−34 %↓
RuCM18-CSF-M2	26.8	33.4	−25 %↓	−34 %↓
RuCM18-CSF-L1	27.0	35.5	−24 %↓	−30 %↓
RuCM18-CSF-L2	15.5	28.0	−56 %↓	−45 %↓
RuCM27	19.7	30.2	0 %	0 %
RuCM27-WTSF1	21.9	26.4	11 %↑	−13 %↓
RuCM27-WTSF2	24.0	34.0	22 %↑	13 %↑
RuCM27-CSF-M1	22.3	28.8	13 %↑	−5 %↓
RuCM27-CSF-M2	23.0	32.8	17 %↑	9 %↑
RuCM36	14.3	22.4	0 %	0 %
RuCM36-WTSF1	17.6	26.6	23 %↑	19 %↑
RuCM36-WTSF2	15.8	28.9	10 %↑	29 %↑
RuCM36-CSF-M1	18.0	22.9	26 %↑	2 %↑
RuCM36-CSF-M2	14.8	25.6	4 %↑	14 %↑

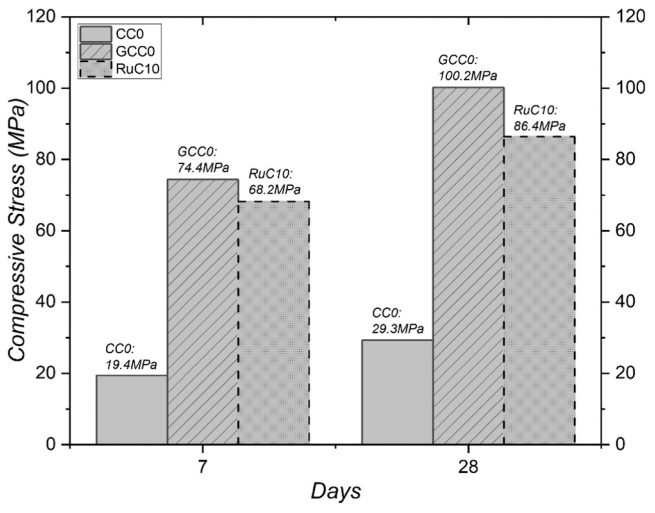

Fig. 5. Compressive strengths of RuC mix incorporating SCMs with and without WTR.

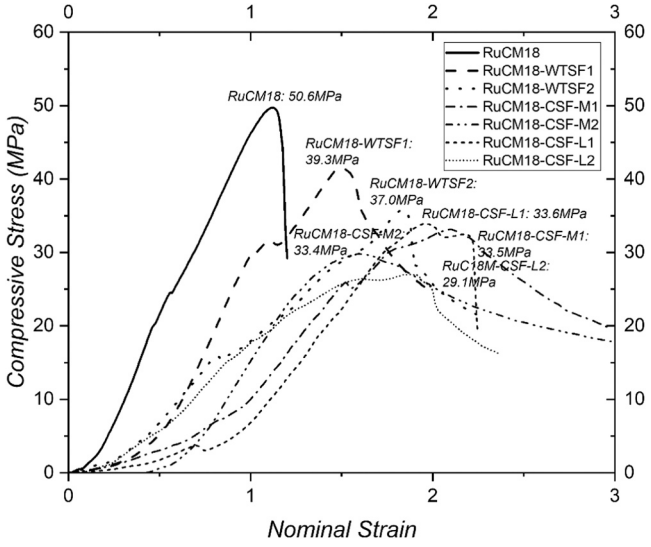

Fig. 6. Difference in mortar compressive strengths (at 28-days) with WTSF and CSF at 18 % WTR volumetric replacement.

The stress-strain curves derived from specimens containing 18 % rubber particles are depicted in Fig. 6. It is hypotheses from the illustration that the inclusion of fibre material diminishes the homogeneity of the mix, thereby leading to a decline in both strength and modulus. Particularly, the compressive strength experiences more deterioration when fibres of similar lengths and thicknesses are utilized, compared to fibres with varying lengths and thicknesses. This observation further highlights that shorter fibres are more effective in compression than longer fibres, contributing to the nuanced behaviour of the composite material under stress.

For specimens with higher WTR content at 27 % and 36 %, as depicted in stress-strain curves illustrated in Figs. 7 and 8, it is evident that fibre reinforcement effectively mitigated the brittleness of the matrix. Medina [70] reported that small percentages of rubber can enhance the toughness and fire spalling resistance of concrete. While increasing the rubber percentage generally reduces concrete strength, this reduction can be mitigated by adding fibres, latex, or fillers. This delay in the formation of macro cracks contributed to the overall improvement in strength and modulus of the composite material. Notably, the most favourable strength gains were observed for 36 % WTR replacement. With the addition of WTSF2, there was a remarkable 29 % increase in compressive strength as compared to the base mix, surpassing the improvement achieved with CSF-M2 by 14 %.

3.1.4. Concrete incorporating steel fibres

The assessment of RuC mix reinforced with WTSF reveals a consistent decrease in compressive strength with an increase in WTSF proportion. The addition of 1 % WTSF denoted as 'WTSF1' leads to a 13 % reduction (74.8 MPa), and the subsequent inclusion of 2 % WTSF denoted as 'WTSF2' results in a further 20 % decrease (69.5 MPa). Surprisingly, the addition of 3 % WTSF denoted as 'WTSF3' shows a slight 9 % improvement as compared to WTSF2, yet still experiences an 11 % reduction in compressive strength (76.6 MPa) when compared to the base optimised RuC mix with 10 % WTR replacement without the addition of WTSF (86.4 MPa), as detailed in Table 7. This reduction in strength might be due to the impact of WTSF on the homogeneity and bonding of the mix matrix. The adhesion between WTSF and the concrete matrix likely disrupted the mix, leading to decreased strength. This deterioration continued with further additions of WTSF up to 2 %. However, when 3 % WTSF was added, there was an unexpected 9 % improvement. This improvement could be due to several factors. First, it might have reached the minimum required dosage of steel fibres in the concrete specimen, compensating for the negative impact of WTSF supplementation. Second, the thorough mixing of 3 % WTSF in the concrete mix, though challenging, and may have resulted in some extended entanglement of the steel fibres. This large number of entanglements could have allowed the fibres to settle in a series aligned perpendicular to the load, enhancing the strength without significantly compromising the bonding of the concrete matrix. As a result, this configuration led to a slight improvement in compressive strength compared to the strengths observed with up to 2 % WTSF additions.

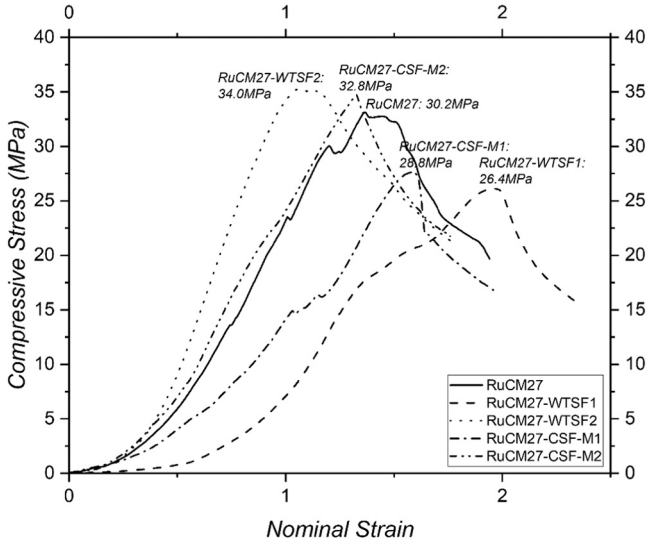

Fig. 7. Difference in compressive strengths (at 28-days) with WTSF and CSF-M at 27 % WTR volumetric replacement.

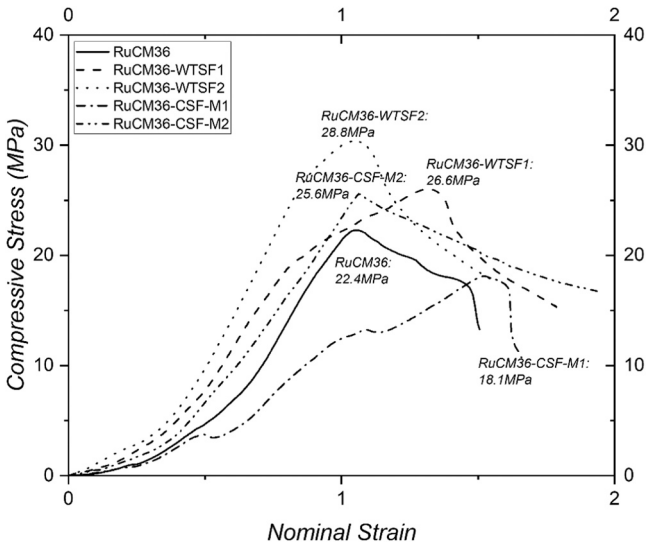

Fig. 8. Difference in compressive strengths (at 28-days) with WTSF and CSF-M at 36 % WTR volumetric replacement.

Table 7
Compressive strengths of RuC mix incorporating WTR reinforced with WTSF.

Concrete Type	fc' (MPa)		% Increase/ Decrease With reference to RuC10	
	at 7-days	at 28-days	at 7-days	at 28-days
RuC10	68.2	86.4	0 %	0 %
RuC10-WTSF1	62.3	74.8	−9 %↓	−13 %↓
RuC10-WTSF2	63.6	69.5	−7 %↓	−20 %↓
RuC10-WTSF3	60.6	76.6	−11 %↓	−11 %↓

However, Eisa, Ahmed S, et al. [71] found that using WTR as a partial replacement for fine aggregates at 5–10 % showed good mechanical properties, though it led to a reduction in compressive strength by 10 % and 24 %, respectively.

3.2. Flexural-tensile performance

3.2.1. Mortar

The flexural performance of the mortar mixtures with 18 % volumetric rubber particle content are summarised in Table 8.

The test results indicated a reduction of 27 %, 17 %, and 8 % at 28 days, respectively, for WTR sizes between Ø2–4 mm, Ø0.7–2.0 mm, and Ø0.2–2.0 mm, compared to the particle size ranging between Ø0.2–0.7 mm denoted as optimised RuCM18- Ø0.2–0.7 mm. The flexural strength for fine particles in the size range of Ø0.2–0.7 mm reached up to 9.4 MPa at 28 days, in contrast to 6.9 MPa for coarse particle sizes varying between Ø2–4 mm. Fig. 9 depicts the comparison of flexural strength variation for different WTR particle size ranges through a stress-deflection curve.

Similar to the observed trend in compressive strength, an increase in WTR dosage from 18 % (referred as 'RuCM18') to 54 % (referred as

Table 8
Effect of WTR particle size variations on flexural strength of RuC mortar mix.

Mortar Sample	fr (MPa)		% Increase/ Decrease		
			fr	With reference to RuCM18–Ø0.2–0.7 mm	
	at 7-days	at 28-days	at 28-days	at 7-days	at 28-days
RuCM18-Ø0.2–0.7 mm	6.9	9.4	36 %↑	0 %	0 %
RuCM18-Ø0.2–2 mm	6.8	8.6	28 %↑	−2 %↓	−8 %↓
RuCM18-Ø0.7–2 mm	5.6	7.8	40 %↑	−19 %↓	−17 %↓
RuCM18-Ø2–4 mm	6.4	6.9	7 %↑	−7 %↓	−27 %↓

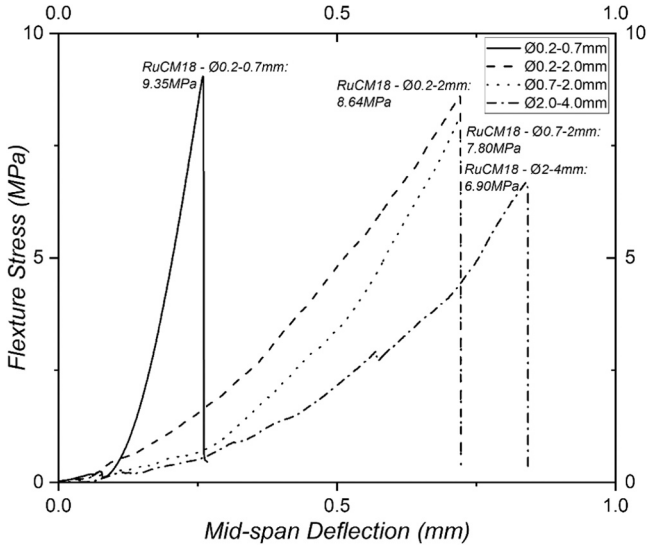

Fig. 9. Comparison of reduction in flexural strengths (at 28-days) with different WTR particle sizes.

'RuCM54') results in a reduction in flexural strength. The impact of WTR content on flexural characteristics is summarised in Table 9.

The results pertaining to the three-point bending strength of RuCM mix specimens, following 28 days of curing, are depicted in Fig. 10. Notably, the flexural strength performance mirrors the trends observed in compressive strength, both demonstrating a decline with increasing WTR dosage. However, this decrease is more accentuated in compressive strength as compared to flexural strength, particularly evident at higher WTR dosage replacements. These findings, illustrated in the stress-deflection curve presented in Fig. 10, underscore the nuanced mechanical behavior of RuCM mixes under varying WTR dosages. This is

Table 9
Flexural strengths of RuC mortar mix incorporating WTR.

Mortar Sample	fr (MPa)		% Increase/ Decrease		
			fr	With reference to RuCM18	
	at 7-days	at 28-days	at 28-days	at 7-days	at 28-days
CM0	6.8	10.4	52 %↑	−0.9 %↓	10.7 %↑
GCM0	4.8	9.4	96 %↑	−30.4 %↓	0.0 %
RuCM9	5.1	7.2	41 %↑	−26.1 %↓	−23.4 %↓
RuCM18	6.9	9.4	36 %↑	0.0 %	0.0 %
RuCM27	5.4	7.8	44 %↑	−21.7 %↓	−17.0 %↓
RuCM36	4.4	6.5	48 %↑	−36.2 %↓	−30.9 %↓
RuCM54	3.8	5.4	42 %↑	−44.9 %↓	−42.6 %↓

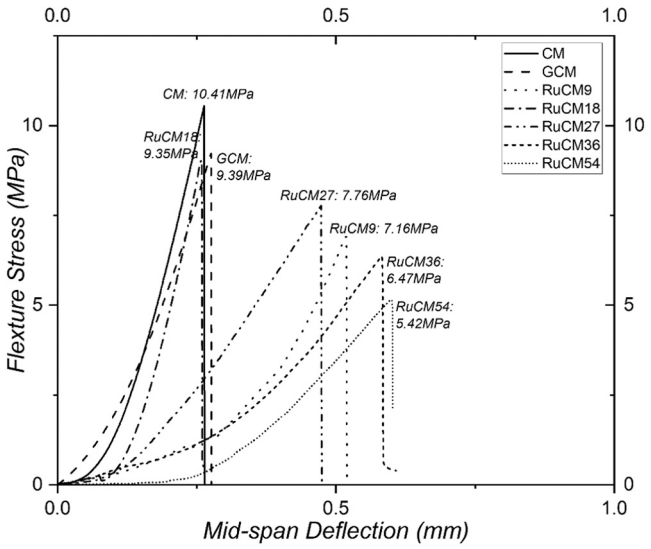

Fig. 10. Variation in flexural strengths (at 28-days) with different WTR particle proportions (0 %, 9 %, 18 %, 27 %, 36 %, 54 %).

attributed to the weak connection between cement paste and WTR particles [72].

3.2.2. Concrete

The optimized RuC mix with 10 % WTR volumetric replacement, denoted as 'RuC10', showcases significant improvements in mechanical properties compared to the base CC mix without any WTR replacement, labeled as 'CC0'. Specifically, RuC10 demonstrates a notable 61 % increase in flexural strength (9.0 MPa versus 5.6 MPa). In contrast, the GCC mix, also without any WTR inclusion and denoted as 'GCC0', exhibits only a slight increase in flexural strength (9.4 MPa versus 9.0 MPa) compared to RuC10, as shown in Table 10. These findings underscore the superior flexure performance of RuC10. Further supporting evidence is provided by Bensaci, Hamza et. al. [73] through their experimental investigation focusing on the production of self-consolidating Rubberised concrete (SCRuC) using either WTR or WTSF. The study involved replacing natural aggregates with WTR particles by volume ranging from 0 % to 30 %. Additionally, WTSF were incorporated into SCRuC mixes at volume fractions ranging from 0.5 % to 1.5 %. The experimental findings reveal that the addition of WTSF positively impacts the SCC, resulting in increased flexural strength and reduced shrinkage and risk of cracking.

3.2.3. Mortar incorporating steel fibres

This study meticulously explored the effects of WTSF and CSF reinforcement, with varying volumetric fractions up to 2 %. The numeric annotation '1' signifies a 1 % addition of steel fibres, while '2' denotes a 2 % addition, as indicated at the end of WTSF, CSF-M, and CSF-L. The investigation specifically targeted the flexural strength of RuC mortar mixes, each characterized by different levels of WTR replacement.

Table 10
Flexural strengths of RuC mix incorporating WTR.

Concrete Sample	fr (MPa)		% Increase/ Decrease		
			fr	With reference to RuC10	
	at 7-days	at 28-days	at 28-days	at 7-days	at 28-days
CC0	4.7	5.6	18 %↑	−35 %↓	−38 %↓
GCC0	7.9	9.4	19 %↑	10 %↑	4 %↑
RuC10	7.2	9.0	25 %↑	0 %	0 %

Table 11
Flexural strengths of RuC Mortar mix incorporating WTR reinforced with WTSF and CSF.

Mortar Sample	fr (MPa)		% Increase/ Decrease	
			With reference to RuCM18, RuCM27 and RuCM36, respectively.	
	at 7-days	at 28-days	at 7-days	at 28-days
RuCM18	4.8	9.4	0 %	0 %
RuCM18-WTSF1	7.1	8.5	48 %↑	−10 %↓
RuCM18-WTSF2	12.1	15.5	153 %↑	65 %↑
RuCM18-CSF-M1	7.8	9.2	63 %↑	−2 %↓
RuCM18-CSF-M2	13.6	15.8	182 %↑	68 %↑
RuCM18-CSF-L1	9.8	13.5	105 %↑	44 %↑
RuCM18-CSF-L2	14.0	17.0	193 %↑	81 %↑
RuCM27	5.4	7.8	0 %	0 %
RuCM27-WTSF1	7.2	8.0	34 %↑	3 %↑
RuCM27-WTSF2	9.0	13.9	66 %↑	79 %↑
RuCM27-CSF-M1	9.1	9.2	68 %↑	18 %↑
RuCM27-CSF-M2	11.8	14.0	118 %↑	80 %↑
RuCM36	4.4	6.5	0 %	0 %
RuCM36-WTSF1	6.3	7.8	43 %↑	21 %↑
RuCM36-WTSF2	8.2	9.0	85 %↑	39 %↑
RuCM36-CSF-M1	7.0	8.1	58 %↑	26 %↑
RuCM36-CSF-M2	10.4	11.1	137 %↑	71 %↑

Table 11 demonstrates that a reinforcement of steel fibres provides evident flexures strength enhancement across all mixtures.

The inclusion of WTSF2 and CSF-M2 demonstrated similar outcomes for RuCM18 and RuCM27 mixtures. However, the introduction of CSF-L2 resulted in a notable enhancement of flexural strength, approximately 10 % higher than that achieved with WTSF2, in the RuC mortar mix featuring 18 % WTR volumetric replacement (referred to as 'RuCM18'). It's worth noting that while WTSF fibres showcased superior reinforcement effects in compressive behaviour, CSF-L fibres exhibited the highest reinforcement effect in flexural tests, attributed to their longer length and aspect ratio as compared to the other fibre types tested in this study. CSF-L fibres, being hooked-end high-tensile-strength fibres, have a length of 50 mm, a diameter of 1.0 mm, an aspect ratio of 60, and with a tensile strength of 1900 N/mm^2. In contrast with WTSF fibres have varying disoriented uneven bended lengths from 25–50 mm and thicknesses ranging from 0.15–0.40 mm, with diverse tensile strengths and aspect ratios, however CSF-M fibres, were single-hooked, measure 35 mm in length, 0.55 mm in diameter, have an aspect ratio of 65, and a tensile strength of 1345 N/mm^2.

The superior performance of CSF-L fibres in flexural tests is likely due to their longer length, thick diameter, and higher tensile strength, allowing them to hold macro cracks and absorb more energy during loading. These fibres due to their characteristics able to settle more in alignment that is perpendicular to the direction of the load, which enhances their flexural strength performance. Additionally, the aspect ratio of 60 for CSF-L fibres, while slightly lower than the 65 for CSF-M fibres, contributes to their overall effectiveness in improving flexural strength due to the combined effects of length, diameter, and tensile strength, when compared to the other fibre types tested in this study.

This finding is supported by research conducted by M.A. Aiello et al. [19] which showed that the post-cracking behaviour of WTSF reinforced concrete, as determined by flexural tests, was comparable to that of CSF reinforced concrete. WTSF reinforced concrete specimens exhibited good energy absorption and maintained good residual strength after cracking.

Figs. 11 and 12 provide additional insight into the stress-deflection curve, indicating that the inclusion of fibre material enhance the loading capacity i.e. the flexural strength of RuC mortar mix.

3.2.4. Concrete incorporating steel fibres

The addition of WTSF1 led to a 6 % increase in flexural strength (9.5 MPa), while WTSF2 resulted in a more substantial 15 % increase (10.3 MPa). Notably, WTSF3 achieved the highest improvement, with a remarkable 38 % increase (12.4 MPa), as compared to the flexural strength (9.0 MPa) of the RuC base mix with 10 % WTR replacement, denoted as 'RuC10', without any WTSF addition, as illustrated in Table 12.

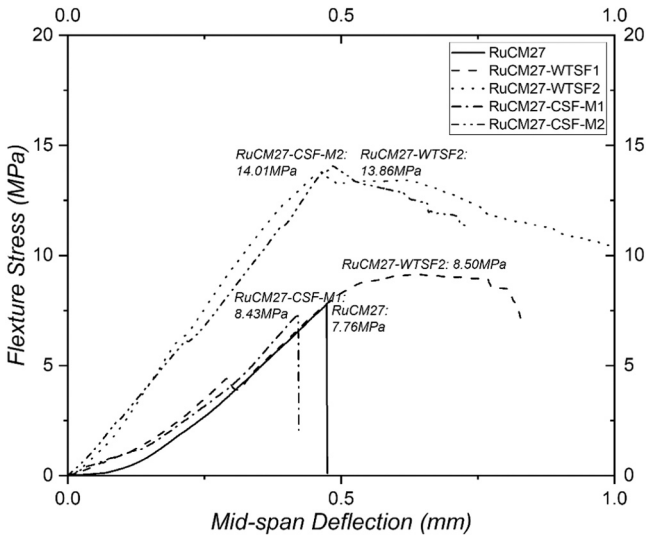

Fig. 11. Difference in compressive strengths (at 28-days) with WTSF and CSF at 27 % WTR volumetric replacement.

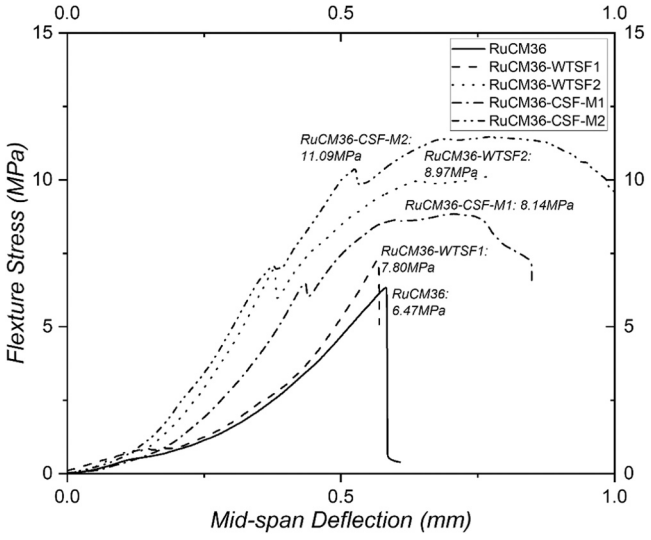

Fig. 12. Difference in compressive strengths (at 28-days) with WTSF and CSF at 36 % WTR volumetric replacement.

Table 12
Flexural strengths of RuC mix incorporating WTR reinforced with WTSF.

Concrete Type	fr (MPa)		% Increase/ Decrease	
			With reference to RuC10	
	at 7-days	at 28-days	at 7-days	at 28-days
RuC10	7.2	9.0	0 %	0 %
RuC10-WTSF1	7.4	9.5	3 %↑	6 %↑
RuC10-WTSF2	7.3	10.3	2 %↑	15 %↑
RuC10-WTSF3	8.9	12.4	24 %↑	38 %↑

4. Conclusion

In conclusion, this study provides a comprehensive analysis of the mechanical characteristics of an eco-friendly RuC in which the 63 % of cement is partially replaced by GGBS and FA, and high amount of WTR is used to replace natural sand as the aggregates, however matrix is further reinforced with WTSF. The key findings can be drawn as follows:

1) Water treated finer WTR particles demonstrate superior cohesion with fewer voids, leading to a remarkable 68 % increase in compressive strength and a 27 % rise in flexural strength as compared to medium and coarse particles. However, as the proportion of WTR substitution increases, there is a significant decrease in compressive strength by approximately 77 % and flexural strength by up to 43 % with up to 54 % WTR replacement. Nonetheless, this increase in WTR substitution enhances ductility, enabling the specimens to withstand loads for an extended period.
2) 18 % WTR in RuC mortar mix demonstrates approximately 12 % higher compressive and 31 % higher flexural strengths as compared to a lower replacement percentage of 9 %. This difference underscores the importance of achieving an optimal replacement level, as insufficient mixing at lower replacement percentages can result in decreased mechanical properties.
3) Despite experiencing a 23 % reduction in compressive strength, the optimized RuCM18 mix maintains its flexural strength, indicating uniform distribution of WTR and successful integration with the mortar matrix.
4) The inclusion of WTSF in the optimized RuCM18 mix has a significant impact on both compressive and flexural strengths. With a 2 % WTSF addition, there is a decrease in compressive strength by 27 %, but a 65 % increase in flexural strength. For higher WTR replacement mixes such as RuCM27 and RuCM36, with 2 % WTSF additions enhances compressive strength marginally and evidently in flexural strength.
5) The optimized RuC10 mix with 3 % WTSF additions exhibits an 11 % reduction in compressive strength but exhibits a notable enhancement of 38 % in flexural strength. The WTSF fibre demonstrates close performance to commercially available new fibres.

Author statement

The authors affirm that all research was conducted in accordance with relevant ethical guidelines and regulations, and appropriate permissions were obtained where necessary.

CRediT authorship contribution statement

Daichao Sheng: Writing – review & editing. **Muneeb Qureshi:** Writing – original draft, Formal analysis. **Chengqing Wu:** Writing – review & editing. **Jun Li:** Writing – review & editing, Supervision, Resources, Project administration, Funding acquisition, Conceptualization.

Declaration of Competing Interest

The authors declare that there is no conflict of interest.

Data availability

Data will be made available on request.

Acknowledgement

Australian Research Council Linkage Project LP220200796 is supporting this project.Raw rubber and recycled fibre material are supplied by Tyrex from Sydney, the authors appreciate their support.

References

[1] S. Mindess, Developments in the Formulation and Reinforcement of Concrete, Woodhead Publishing, 2019.
[2] N.N. Eldin, A.B. Senouci, Observations on rubberized concrete behavior, Cem., Concr. Aggreg. 15 (1) (1993).
[3] T.M. Pham, N. Renaud, V.L. Pang, F. Shi, H. Hao, W. Chen, Effect of rubber aggregate size on static and dynamic compressive properties of rubberized concrete, Struct. Concr. 23 (4) (2022) 2510–2522.
[4] A.R. Khaloo, M. Dehestani, P. Rahmatabadi, Mechanical properties of concrete containing a high volume of tire–rubber particles, Waste Manag. 28 (12) (2008) 2472–2482.
[5] J. Ahmad, Z. Zhou, A. Majdi, M. Alqurashi, A.F. Deifalla, Overview of concrete performance made with waste rubber tires: a step toward sustainable concrete, Materials 15 (16) (2022) 5518.
[6] K.B. Najim, M.R. Hall, Mechanical and dynamic properties of self-compacting crumb rubber modified concrete, Constr. Build. Mater. 27 (1) (2012) 521–530.
[7] E. Ozbay, M. Lachemi, U.K. Sevim, Compressive strength, abrasion resistance and energy absorption capacity of rubberized concretes with and without slag, Mater. Struct. 44 (2011) 1297–1307.
[8] B.S. Thomas, R.C. Gupta, Properties of high strength concrete containing scrap tire rubber, J. Clean. Prod. 113 (2016) 86–92.
[9] M.M. Reda Taha, A.S. El-Dieb, M.A. Abd Al-Wahab, M.E. Abdel-Hameed, Mechanical, fracture, and microstructural investigations of rubber concrete, J. Mater. Civ. Eng. 20 (10) (2008) 640–649.
[10] T. Gupta, S. Chaudhary, R.K. Sharma, Assessment of mechanical and durability properties of concrete containing waste rubber tire as fine aggregate, Constr. Build. Mater. 73 (2014) 562–574.
[11] R. Roychand, R.J. Gravina, Y. Zhuge, Z. Ma, J.E. Mills, O. Youssf, Practical rubber pre-treatment approch for concrete use—an experimental study, J. Compos. Sci. 5 (6) (2021) 143.
[12] S. Raffoul, R. Garcia, K. Pilakoutas, M. Guadagnini, N.F. Medina, Optimisation of rubberised concrete with high rubber content: an experimental investigation, Constr. Build. Mater. 124 (2016) 391–404.
[13] M. Turki, I.Z. Estelle Bretagne, M. Quéneudec, Influence of filler addition on mechanical behavior of cementitious mortar-rubber aggregates: experimental study and modeling. J. Mater. Civ. Eng. 24 (11) (2012) 1350–1358.
[14] J. Xie, C. Fang, Z. Lu, Z. Li, L. Li, Effects of the addition of silica fume and rubber particles on the compressive behaviour of recycled aggregate concrete with steel fibres, J. Clean. Prod. 197 (2018) 656–667.
[15] A. Siddika, M.A. Al Mamun, R. Alyousef, Y.H. Mugahed Amran, F. Aslani, H. Alabduljabbar, Properties and utilizations of waste tire rubber in concrete: a review, Constr. Build. Mater. 224 (2019) 711–731.
[16] R. Bušić, M. Benšić, I. Miličević, K. Strukar, Prediction models for the mechanical properties of self-compacting concrete with recycled rubber and silica fume, Materials 13 (8) (2020) 1821.
[17] Z. Chen, L. Li, Z. Xiong, Investigation on the interfacial behaviour between the rubber-cement matrix of the rubberized concrete, J. Clean. Prod. 209 (2019) 1354–1364.
[18] Bedewi, N., Steel fiber reinforced concrete made with fibers extracted from used tyres. Energy, Master's thesis in Civil Engineering, Addis Ababa University, Addis Ababa, Ethiopia, 2009.
[19] M.A. Aiello, F. Leuzzi, G. Centonze, A. Maffezzoli, Use of steel fibres recovered from waste tyres as reinforcement in concrete: pull-out behaviour, compressive and flexural strength, Waste Manag. 29 (6) (2009) 1960–1970.
[20] Ş. Yazıcı, G. İnan, V. Tabak, Effect of aspect ratio and volume fraction of steel fiber on the mechanical properties of SFRC, Constr. Build. Mater. 21 (6) (2007) 1250–1253.
[21] C.D. Atiş, O. Karahan, Properties of steel fiber reinforced fly ash concrete, Constr. Build. Mater. 23 (1) (2009) 392–399.
[22] S.S.M. Samarakoon, P. Ruben, J.W. Pedersen, L. Evangelista, Mechanical performance of concrete made of steel fibers from tire waste, Case Stud. Constr. Mater. 11 (2019) e00259.
[23] J. Tejchman, J. Kozicki, Experimental and theoretical investigations of steel-fibrous concrete, Vol. 3, Springer, 2010.
[24] C.G. Papakonstantinou, M.J. Tobolski, Use of waste tire steel beads in Portland cement concrete, Cem. Concr. Res. 36 (9) (2006) 1686–1691.
[25] P. Bhargava, U.K. Sharma, S.K. Kaushik, Compressive stress-strain behavior of small scale steel fibre reinforced high strength concrete cylinders, J. Adv. Concr. Technol. 4 (1) (2006) 109–121.
[26] K. Aghaee, M.A. Yazdi, K.D. Tsavdaridis, Investigation into the mechanical properties of structural lightweight concrete reinforced with waste steel wires, Mag. Concr. Res. 67 (4) (2015) 197–205.
[27] O.A. Abaza, Z.S. Hussein, Flexural behavior of steel fiber-reinforced rubberized concrete, J. Mater. Civ. Eng. 28 (1) (2016) 04015076.
[28] Y. Park, A. Abolmaali, M. Mohammadagha, S.-H. Lee, Flexural characteristic of rubberized hybrid concrete reinforced with steel and synthetic fibers, Adv. Civ. Eng. Mater. 3 (1) (2014) 495–508.
[29] A. Turatsinze, J.-L. Granju, S. Bonnet, Positive synergy between steel-fibres and rubber aggregates: effect on the resistance of cement-based mortars to shrinkage cracking, Cem. Concr. Res. 36 (9) (2006) 1692–1697.
[30] A.T. Noaman, B.A. Bakar, H.M. Akil, Experimental investigation on compression toughness of rubberized steel fibre concrete, Constr. Build. Mater. 115 (2016) 163–170.

[31] J. NdayambajeStructural performance and impact resistance of rubberized concrete2018ASTM International5, Structural performance and impact resistance of rubberized concrete.
[32] K. Pilakoutas, K. Neocleous, H. Tlemat, Reuse of tyre steel fibres as concrete reinforcement. in Proceedings of the Institution of Civil Engineers-Engineering Sustainability, Thomas Telford Ltd, 2004.
[33] H. Hu, P. Papastergiou, H. Angelakopoulos, M. Guadagnini, K. Pilakoutas, Mechanical properties of SFRC using blended manufactured and recycled tyre steel fibres, Constr. Build. Mater. 163 (2018) 376–389.
[34] A.G. Graeff, K. Pilakoutas, K. Neocleous, N.N. Peres, M.V., Fatigue resistance and cracking mechanism of concrete pavements reinforced with recycled steel fibres recovered from post-consumer tyres, Eng. Struct. 45 (2012) 385–395.
[35] L. Pan, H. Hao, J. Cui, T.M. Pham, Numerical study on dynamic properties of rubberised concrete with different rubber contents, Def. Technol. 24 (2023) 228–240.
[36] T.M. Pham, W. Chen, A.M. Khan, H. Hao, M. Elchalakani, T.M. Tran, Dynamic compressive properties of lightweight rubberized concrete, Constr. Build. Mater. 238 (2020) 117705.
[37] T.M. Pham, J. Liu, P. Tran, V.-L. Pang, F. Shi, W. Chen, H. Hao, T.M. Tran, Dynamic compressive properties of lightweight rubberized geopolymer concrete, Constr. Build. Mater. 265 (2020) 120753.
[38] T.M. Pham, J. Davis, N. San Ha, E. Pournasiri, F. Shi, H. Hao, Experimental investigation on dynamic properties of ultra-high-performance rubberized concrete (UHPRuC), Constr. Build. Mater. 307 (2021) 125104.
[39] T. Awolusi, O.L. Oke, O.O. Akinkurolere, A.O. Sojobi, Application of response surface methodology: Predicting and optimizing the properties of concrete containing steel fibre extracted from waste tires with limestone powder as filler, Case Stud. Constr. Mater. 10 (2019) e00212.
[40] F. De Larrard, T. Sedran, Optimization of ultra-high-performance concrete by the use of a packing model, Cem. Concr. Res. 24 (6) (1994) 997–1009.
[41] F. De Larrard, T. Sedran, Mixture-proportioning of high-performance concrete, Cem. Concr. Res. 32 (11) (2002) 1699–1704.
[42] W.B. Fuller, S.E. Thompson, The laws of proportioning concrete, Trans. Am. Soc. Civ. Eng. 59 (2) (1907) 67–143.
[43] T. Saidi, M. Hasan, A.D.D. Riski, R.R. Ayunizar, A. Mubarak, Mix design and properties of reactive powder concrete with diatomaceous earth as cement replacement. in IOP Conference Series: Materials Science and Engineering, IOP Publishing, 2020.
[44] J.E. Funk, D.R. Dinger, Predictive process control of crowded particulate suspensions: applied to ceramic manufacturing, Springer Science & Business Media, 2013.
[45] Hüsken, G., *A multifunctional design approach for sustainable concrete: with application to concrete mass products*. 2010.
[46] H. Brouwers, Particle-size distribution and packing fraction of geometric random packings, Phys. Rev. E 74 (3) (2006) 031309.
[47] Hunger, M., *An integral design concept for ecological self-compacting concrete*. 2010: University of Technology.
[48] J. Chen, A. Kwan, Superfine cement for improving packing density, rheology and strength of cement paste, Cem. Concr. Compos. 34 (1) (2012) 1–10.
[49] A. Kwan, J. Chen, Adding fly ash microsphere to improve packing density, flowability and strength of cement paste, Powder Technol. 234 (2013) 19–25.
[50] F. De Larrard, Concrete mixture proportioning: a scientific approach, CRC Press, 1999.
[51] C. Gong, L. Kang, M. Cheng, M. Lei, Parameter modification and extension of the compressible packing model (CPM) for steel fiber-aggregate mixtures, Powder Technol. 422 (2023) 118479.
[52] P.M. Bartos, C. Hoy, Interaction of particles in fibre reinforced concrete. in Production methods and workability of concrete, CRC Press, 2004, pp. 463–474.
[53] C. Gong, L. Kang, L. Liu, M. Lei, W. Ding, Z. Yang, A novel prediction model of packing density for single and hybrid steel fiber-aggregate mixtures, Powder Technol. 418 (2023) 118295.
[54] E. Ganjian, M. Khorami, A.A. Maghsoudi, Scrap-tyre-rubber replacement for aggregate and filler in concrete, Constr. Build. Mater. 23 (5) (2009) 1828–1836.
[55] C.A. Issa, G. Salem, Utilization of recycled crumb rubber as fine aggregates in concrete mix design, Constr. Build. Mater. 42 (2013) 48–52.
[56] B.S. Thomas, R.C. Gupta, Long term behaviour of cement concrete containing discarded tire rubber, J. Clean. Prod. 102 (2015) 78–87.
[57] T.M. Pham, M. Elchalakani, H. Hao, J. Lai, S. Ameduri, T.M. Tran, Durability characteristics of lightweight rubberized concrete, Constr. Build. Mater. 224 (2019) 584–599.
[58] T.M. Pham, Y.Y. Lim, M. Malekzadeh, Effect of pre-treatment methods of crumb rubber on strength, permeability and acid attack resistance of rubberised geopolymer concrete, J. Build. Eng. 41 (2021) 102448.
[59] Johansson, A. *The relationship between mixing time and type of concrete mixer*. in *Swedish Cement Concr Inst Proc*. 1971.
[60] C.F. Ferraris, Concrete mixing methods and concrete mixers: state of the art, J. Res. Natl. Inst. Stand. Technol. 106 (2) (2001) 391.
[61] L. Pan, H. Hao, J. Cui, T.M. Pham, Numerical study on impact resistance of rubberised concrete roadside barrier, Adv. Struct. Eng. 26 (1) (2023) 17–35.
[62] H. Su, J. Yang, T.C. Ling, G.S. Ghataora, S. Dirar, Properties of concrete prepared with waste tyre rubber particles of uniform and varying sizes, J. Clean. Prod. 91 (2015) 288–296.
[63] H.S. Lee, H. Lee, J.S. Moon, H.W. Jung, Development of tire added latex concrete, Mater. J. 95 (4) (1998) 356–364.
[64] T. Du, Y. Yang, H. Cao, N. Si, H. Kordestani, Z.D.I. Sktani, A. Arab, C. Zhang, Rubberized concrete: effect of the rubber size and content on static and dynamic behavior, Buildings 14 (6) (2024) 1541.
[65] Z.K. Khatib, F.M. Bayomy, Rubberized Portland cement concrete, J. Mater. Civ. Eng. 11 (3) (1999) 206–213.
[66] K.H. Chung, Y.K. Hong, Introductory behavior of rubber concrete, J. Appl. Polym. Sci. 72 (1) (1999) 35–40.
[67] W. Huang, X. Huang, Q. Xing, Z. Zhou, Strength reduction factor of crumb rubber as fine aggregate replacement in concrete, J. Build. Eng. 32 (2020) 101346.
[68] L. Li, S. Ruan, L. Zeng, Mechanical properties and constitutive equations of concrete containing a low volume of tire rubber particles, Constr. Build. Mater. 70 (2014) 291–308.
[69] Z. Wu, C. Shi, W. He, L. Wu, Effects of steel fiber content and shape on mechanical properties of ultra high performance concrete, Constr. Build. Mater. 103 (2016) 8–14.
[70] N.F. Medina, R. Garcia, I. Hajirasouliha, K. Pilakoutas, M. Guadagnini, S. Raffoul, Composites with recycled rubber aggregates: properties and opportunities in construction, Constr. Build. Mater. 188 (2018) 884–897.
[71] A.S. Eisa, M.T. Elshazli, M.T. Nawar, Experimental investigation on the effect of using crumb rubber and steel fibers on the structural behavior of reinforced concrete beams, Constr. Build. Mater. 252 (2020) 119078.
[72] R. Roychand, R.J. Gravina, Y. Zhuge, X. Ma, O. Youssf, J.E. Mills, A comprehensive review on the mechanical properties of waste tire rubber concrete, Constr. Build. Mater. 237 (2020) 117651.
[73] H. Bensaci, B. Menadi, S. Kenai, Comparison of some fresh and hardened properties of self-consolidating concrete composites containing rubber and steel fibers recovered from waste tires, Nano Hybrids Compos. 24 (2019) 8–13.